

Moreover, $x = x_0 + \bar{a}_0 t$, x_0 being the value of x at $t = 0$.

If $\bar{\mu}_0 > 0$, an examination of Eq. (33) leads to the conclusion that for $u_{xi}^+ > 0$ (i.e., an expansive wave front), $u_x^+ \rightarrow 0$ as $t \rightarrow \infty$, i.e., the wave decays and damps out ultimately. If $u_{xi}^+ < 0$ (i.e., a compressive wave front), then there exists a positive initial critical value $(u_x^+)_c$ given by

$$(u_x^+)_c = \begin{cases} 2\bar{\mu}_0(\gamma+1)^{-1} & \text{for } j=0 \text{ (plane waves)} \\ \left\{ \left(\frac{\gamma+1}{2} \right) \int_0^\infty (x/x_0)^{-j/2} \exp(-\bar{\mu}_0 t) dt \right\}^{-1} & \text{for cylindrical } (j=1) \text{ and spherical } (j=2) \text{ waves} \end{cases}$$

such that for $|u_{xi}^+| < (u_x^+)_c$, $u_x^+ \rightarrow 0$ as $t \rightarrow \infty$ (i.e., the wave decays ultimately); for $|u_{xi}^+| = (u_x^+)_c$, $u_x^+ \rightarrow 2\bar{\mu}_0(\gamma+1)^{-1}$ as $t \rightarrow \infty$ (i.e., the wave takes a stable wave form); and for $|u_{xi}^+| > (u_x^+)_c$, $|u_x^+| \rightarrow \infty$ as $t \rightarrow t_c$ (i.e., the wave terminates in a shock wave in a finite time) where t_c is given by

$$t_c = (1/\bar{\mu}_0) \log \left\{ 1 + \frac{2\bar{\mu}_0}{(\gamma+1)u_{xi}^+} \right\}^{-1} \quad \text{for } j=0$$

and

$$\int_0^{t_c} (x/x_0)^{-j/2} \exp(-\bar{\mu}_0 t) dt = -2/[(\gamma+1)u_{xi}^+] \quad \text{for } j=1,2$$

One can see from the above expression of $(u_x^+)_c$ that $(\partial(u_x^+)_c/\partial\bar{\mu}_0) > 0$ and $(\partial(u_x^+)_c/\partial x_0) < 0$, which means that the thermal radiation (with $\bar{\mu}_0 > 0$) and the wave-front curvature $(1/x_0)$ both have a stabilizing effect on the tendency of a wave head to grow into a shock in the sense that an increase in $\bar{\mu}_0$ or $(1/x_0)$ causes an increase in $(u_x^+)_c$.

If $\bar{\mu}_0 < 0$, we note that the integral $\int_0^\infty (x/x_0)^{-j/2} \exp(-\bar{\mu}_0 t) dt$ diverges to $+\infty$, and hence the initial critical value of the discontinuity vanishes. Thus Eq. (33) shows that for $\bar{\mu}_0 < 0$, an expansive wave ultimately takes a stable wave form, i.e., for $u_{xi}^+ > 0$, $u_x^+ \rightarrow 2|\bar{\mu}_0|(\gamma+1)^{-1}$ as $t \rightarrow \infty$, while a compressive wave always steepens up into a shock in a finite time, no matter how small the initial discontinuity is, i.e., when $u_{xi}^+ < 0$, $|u_x^+| \rightarrow \infty$ as $t \rightarrow \bar{t}_c$, where \bar{t}_c is given by

$$\bar{t}_c = (1/|\bar{\mu}_0|) \log \left\{ 1 + \frac{2|\bar{\mu}_0|}{(\gamma+1)|u_{xi}^+|} \right\} \quad \text{for } j=0$$

and

$$\int_0^{\bar{t}_c} (x/x_0)^{-j/2} \exp(|\bar{\mu}_0| t) dt = 2/[(\gamma+1)|u_{xi}^+|] \quad \text{for } j=1,2$$

In this case, $(\partial\bar{t}_c/\partial|\bar{\mu}_0|) < 0$ and $(\partial\bar{t}_c/\partial x_0) < 0$, which means that the thermal radiation (with $\bar{\mu}_0 < 0$) causes a compressive wave to steepen into a shock more swiftly than it does in the absence of thermal radiation, whereas an increase in the initial wave-front curvature (x_0^{-1}) delays the shock formation.

References

- Becker, E., "Chemically Reacting Flows," *Annual Review of Fluid Mechanics*, Vol. 4, 1972, pp. 168-175.
- Clarke, J. F. and McChesney, M., *The Dynamics of Relaxing Gases*, Butterworths, London, 1976.
- Srinivasan, J. and Vincenti, W. G., "Criteria for Acoustic Instability in a Gas with Ambient Vibrational and Radiative Nonequilibrium," *Physics of Fluids*, Vol. 18, 1975, pp. 1670-1678.
- Clarke, J. F., "Diffusion Flame Stability," *Combustion Science and Technology*, Vol. 7, 1973, pp. 241-246.

⁵Clarke, J. F., "Behaviour at Acoustic Wave Fronts in a Laminar Diffusion Flame," *Quarterly Journal of Mechanics and Applied Mathematics*, Vol. 27, 1974, pp. 161-173.

⁶Clarke, J. F., "Chemical Amplification at the Wave-Head of a Finite Amplitude Gasdynamic Disturbance," *Journal of Fluid Mechanics*, Vol. 81, 1977, pp. 257-264.

⁷Penner, S. S. and Olfe, D. B., *Radiation and Re-Entry*, Academic Press, New York and London, 1968.

⁸Pai, S. I., "Radiation Gasdynamics: High Temperature Gas Flow Including the Effects of Thermal Radiation," *Mecanique Applique*, Vol. 18, 1973, pp. 813-833.

AIAA 81-4070

Angular Distribution of Radiative Scattering: Comparison of Experiment and Theory

H. F. Nelson*

University of Missouri-Rolla, Rolla, Mo.

Introduction

MEASUREMENT of radiation scattered from suspended matter, which may consist of solid particles, liquid droplets or gas bubbles, is a standard diagnostic technique in the detection of sedimentation, combustion products, atmospheric fallout, flow fields in rocket nozzles, environmental pollution, aerosols, turbine blade lifetime, etc. These measurements are interpreted assuming single scattering and that Mie theory predicts the scattering phase function; consequently, one must be assured that Mie theory and experiment agree. The scattering of radiation by latex spheres has been found to agree roughly with Mie theory.¹ However, only a few investigations have studied the angular distribution of the scattered radiation over a wide range of angles.²⁻⁸ These investigations have used both conventional sources²⁻⁵ and laser sources^{2,6-8} for the incident radiation, but the results were usually obtained for only one value of the particle size parameter^{2,4,7}, or the results emphasized polarization effects.^{6,8} The objective of this Note is to report comparisons of Mie theory and experimental angular scattering of unpolarized radiation for a range of particle size parameters over a large angular range.

The present investigation uses polystyrene latex particles of very narrow size distribution immersed in distilled water to create the scattering medium. The uniform latex particles were obtained from the Dow Chemical Company, Lot Number: 3M4L in a 10% solution by volume. The particles had a mean diameter of 0.481 μm and a standard deviation of 0.0018 μm . The particle solutions were carefully diluted to particle volume concentrations of the order of 10^{-6} for the scattering measurements. A small volume of the emulsifier Triton X-100 was added to the solution to reduce the effects of aggregation.

A Brice-Phoenix light-scattering photometer was used to make the measurements at wavelengths of 0.436, 0.546, and 0.646 μm . The scattered radiation was measured at angles from 40 to 140 deg in 5 deg intervals. The measurements were made using a 26 mm diameter cylindrical cell with flat windows. It had a frosted inside back surface to reduce reflections. The standard narrow 4 mm apertures supplied by the

Received Aug. 15, 1980. Copyright © American Institute of Aeronautics and Astronautics, Inc., 1980. All rights reserved.

*Professor of Aerospace Engineering, Thermal Radiative Transfer Group, Dept. of Mechanical and Aerospace Engineering. Member AIAA.

photometer manufacturer were used to reduce the incident beam width.

Analysis

Experimental

Angular scattering results at a given wavelength are usually presented in terms of the absolute intensity. This is most easily done by defining the absolute intensity ratio in terms of the Rayleigh ratio, $R_{\lambda_0}(\theta)$,⁴ as

$$I_{\lambda_0}(\theta)/I_{\lambda_0}(0) = 4\pi^2 R_{\lambda_0}(\theta)/(N\lambda^2) \quad (1)$$

where N is the number of scattering particles per unit volume, λ is the wavelength of the radiation in the scattering medium and $I_{\lambda_0}(\theta)/I_{\lambda_0}(0)$ is the experimental equivalent of the Mie angular intensity function. Note that $I_{\lambda_0}(0)$ represents the unit intensity incident beam of radiation and not the radiation scattered at $\theta=0$. For uniformly sized scattering particles $N=6\eta/(\pi D^3)$, where D is the particle diameter and η is the volume fraction of scattering particles $\eta = V_{\text{part.}}/(V_{\text{part.}} + V_{\text{water}})$. Therefore, the scattered radiation intensity at angle θ becomes

$$I_{\lambda_0}(\theta)/I_{\lambda_0}(0) = 2(\pi D)^3 R_{\lambda_0}(\theta)/(3\eta\lambda^2) \quad (2)$$

It must be noted that $\lambda = \lambda_0/n_w$ where λ_0 is the vacuum wavelength of the incident beam and n_w is the real part of the index of refraction of water at wavelength λ_0 .

The Rayleigh ratio can be obtained experimentally using the Brice-Phoenix light-scattering photometer. Kratochvil and Smart⁴ discuss a relation of $R_{\lambda_0}(\theta)$ in terms of the geometrical, optical and calibration constants of the Brice-Phoenix light-scattering photometer. The expression which is valid for cylindrical cells with flat entrance and exit windows and a frosted back surface is written as

$$R_{\lambda_0}(\theta) = \left[\frac{TD a n_w^2 R_w/R_c}{1.049\pi h} \right] \sin\theta \left[\frac{(r/r')}{(1-R^2)(1-4R^2)} \right] \left[\frac{D_\theta - 2RD_{(180-\theta)}}{D_\theta}, 1/\text{cm} \right] \quad (3)$$

Where TD is the opal transmission and diffusion correction factor, a is the transmittance of the working standard of the light scattering photometer, R_w/R_c is the dissymmetry correction factor (assumed to be 1.00), h is the width of the primary beam (1.2 cm), r/r' is the narrow beam correction factor (assumed to be 1.3), D_θ is the voltage reading at angle θ , (or at angle $180-\theta$) ratioed to its reading at $\theta=0$ and corrected for the distilled water, and R was calculated from Fresnel's law for perpendicular incidence $R = [(n_c - 1)/(n_c + 1)]^2$ where n_c is the refractive index of the cell at wavelength λ_0 . The values of a , TD , and n_c for the three wavelengths used in this investigation are given in Table 1.

The quantity D_θ represents the voltage G , measured at angle θ divided by the product of the transmittance F of the neutral filters inserted into the incident beam to keep the voltage reading in scale, divided by the same quantity at an angle of zero with the instrument working standard inserted in the beam. In addition, D_θ is corrected by subtracting the distilled water contribution so that

$$D_\theta = \left[\frac{G_\theta}{F_\theta} \frac{F_0}{G_0} \right]_{\text{scattering solution}} - \left[\frac{G_\theta}{F_\theta} \frac{F_0}{G_0} \right]_{\text{distilled water}} \quad (4)$$

A correction for reflection effects at the cell walls is applied to D_θ in Eq. (3) by subtracting $2RD_{(180-\theta)}$ from D_θ and dividing the difference by $(1-R^2)(1-4R^2)$. These reflection

corrections become very important for scattering in the Mie theory regime.

Theoretical

Mie theory allows one to calculate the angular distribution of the scattered intensity for a unit intensity incident beam. The calculations require a knowledge of two input parameters⁹:

- 1) the particle size parameter $x = \pi D n_w / \lambda_0$.
- 2) the scattering particle index of refraction n_p .

The values of x , n_p , and n_w are listed in Table 1 for the three wavelengths of interest.

Results

The scattered radiation intensity ratio is plotted as a function of scattering angle in Figs 1, 2, and 3 at wavelengths of 0.436, 0.546, and 0.646 μm , respectively. The particle volume concentration was 1.0×10^{-6} for all the data. The data was taken twice, first rotating the detector clockwise and second reversing the cell and rotating the detector counterclockwise, in order to reduce the alignment error. The circles represent the average of the two sets of data. The experimental and theoretical results agree very well except at scattering angles greater than about 120 deg. At these large angles the results become very sensitive to the wall reflection correction factor⁴ and to the particle size distribution.^{10,11}

Table 1 Properties

	Wavelength λ_0 , μm		
	0.436	0.546	0.646
x	4.64	3.69	3.11
n_c	1.482	1.474	1.450
n_p	1.621	1.602	1.592
n_w	1.340	1.334	1.331
a	0.0306	0.0394	0.0363
TD	0.280	0.303	0.400

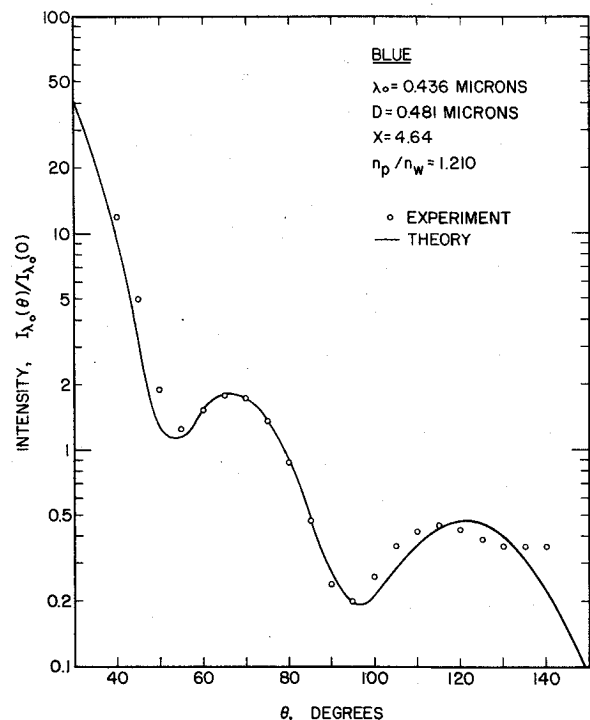


Fig. 1 Comparison of experimental and theoretical angular distribution of scattered radiation for a unit intensity incident beam for $x = 4.64$.

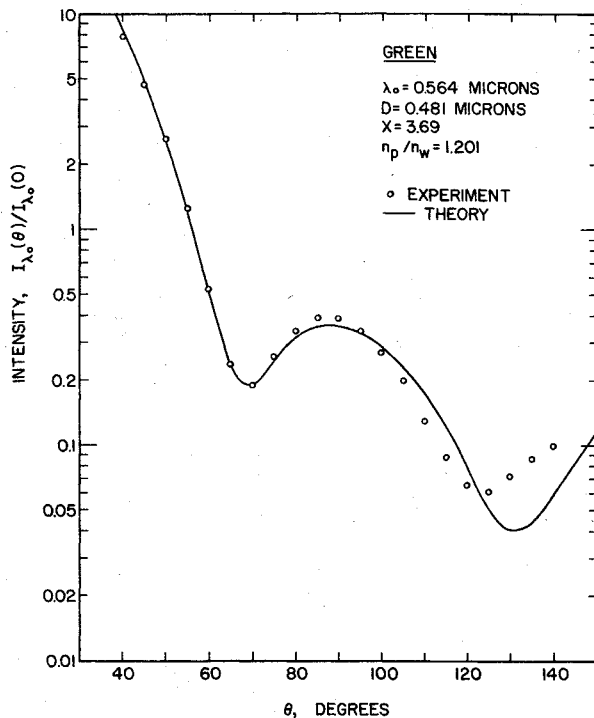


Fig. 2 Comparison of experimental and theoretical angular distribution of scattered radiation for a unit intensity incident beam for $x = 3.69$.

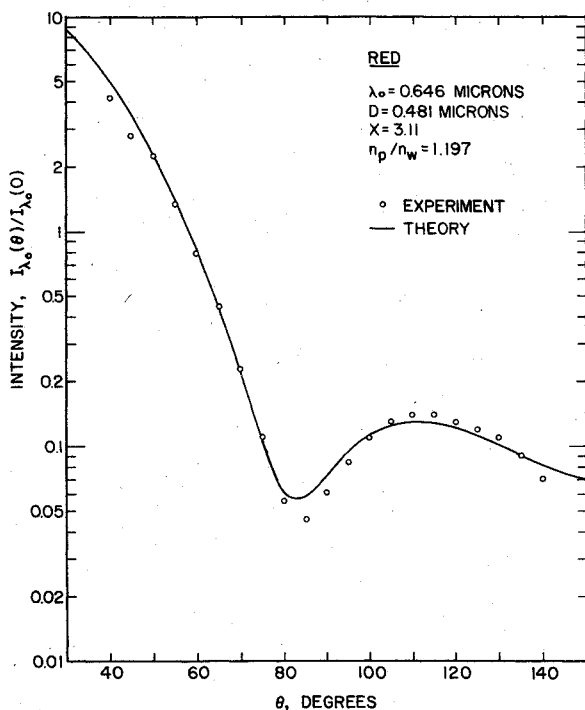


Fig. 3 Comparison of experimental and theoretical angular distribution of scattered radiation for a unit intensity incident beam for $x = 3.11$.

The major contributor to the error in the experimental results is the measurement of η . The measured value of η was increased to 2.5×10^{-6} for all the data to improve the agreement between theory and experiment. Other contributions to the error could be the Rw/Rc factor and the r/r' factor. The values used for these factors were taken from the literature for the instrument.

In the past most of the basic angular scattering work has been published in the colloid and optics literature and has gone unnoticed by the aerospace community. Therefore, the objective of this Note is to point out the good agreement between experiment and Mie theory and bring it to the attention of the aerospace and engineering communities. In addition, the results presented here for three values of the particle size parameter independently reconfirms the good agreement between experiment and theory that has been obtained in the past. This Note also points out the potential for using spherical latex particles of narrow size distribution as scattering particles in controlled laboratory radiation scattering experiments.

Acknowledgment

This work was supported by National Science Foundation Grant ENG 78-07935.

References

- ¹Kerker, M., *The Scattering of Light and Other Electromagnetic Radiation*, Academic Press, New York, N. Y., 1969.
- ²Woodward, D. H., "He-Ne Laser as a Source for Light-Scattering Measurements," *Applied Optics*, Vol. 2, Nov. 1963, pp. 1205-1207.
- ³Dezelic, G. and Kratochvil, J. P., "Determination of Particle Size of Polystyrene Latexes by Light Scattering," *Journal of Colloid Science*, Vol. 16, Dec. 1961, pp. 561-580.
- ⁴Kratochvil, J. P. and Smart, C., "Calibration of Light-Scattering Instruments: III Absolute Angular Intensity Measurements on Mie Scatterers," *Journal of Colloid Science*, Vol. 20, 1965, pp. 875-892.
- ⁵Smart, C., Jacobsen, R., Kerker, M., Kratochvil, J. P., and Matijevic, E., "Experimental Study of Multiple Light Scattering," *Journal of the Optical Society of America*, Vol. 55, Aug. 1965, pp. 947-955.
- ⁶Harris, F. S., Jr., Sherman, G. C., and Morse, F. L., "Experimental Comparison of Scattering of Coherent and Incoherent Light," *IEEE Transactions on Antennas and Propagation*, Vol. AP-15, No. 1, Jan. 1967, pp. 141-147.
- ⁷Colby, P. C., Narducci, L. M., Bluemel, V. and Baer, J., "Light-Scattering Measurements from Dense Optical Systems," *Physical Review A*, Vol. 12, No. 4, Oct. 1975, pp. 1530-1538.
- ⁸Pinnick, R. G., Carroll, D. E. and Hofmann, D. J., "Polarized Light Scattered from Monodisperse Randomly Oriented Nonspherical Aerosol Particles: Measurements," *Applied Optics*, Vol. 15, No. 2, Feb. 1976, pp. 384-393.
- ⁹Look, D. C., "Mie Scattering Computations for Moderately Large Spherical Particles," *Journal of Colloid and Interface Science*, Vol. 56, Aug. 1976, pp. 386-387.
- ¹⁰Wallace, T. P. and Kratochvil, J. P., "Comments on the Comparison of Scattering of Coherent and Incoherent Light by Polydispersed Spheres with Mie Theory," *Applied Optics*, Vol. 8, No. 4, Apr. 1969, pp. 824-826.
- ¹¹Kratochvil, J. P. and Wallace, T. P., "Calibration of Light-Scattering Photometers: VII Calibration by Means of Colloidal Dispersions of Mie Scatterers," *Journal of Physics D: Applied Physics*, Vol. 3, 1970, pp. 221-227.